

ARTICLE OPEN



Influence of the rotation angles on the mechanical behavior of the one reci instrument

Renaud Giess^{1,2}, Éric Mortier^{1,3}, Marie Delanoë⁴, Romain Hocquel⁴, Jean-Marc Martrette^{1,5}, Rémy Balthazard^{1,3} and Marin Vincent^{1,6}

© The Author(s) 2025

AIMS: The reciprocity is a complex endodontic kinematic involving many parameters. The most important of these is undoubtedly the selection of clockwise and counterclockwise rotation angles. In this context, the aim of this study was to determine the influence of clockwise and counterclockwise rotation angles on the mechanical properties of 25/0.06 One Reciprocity instruments.

METHOD: For this purpose, 5 groups of 10 25/0.06 One Reciprocity instruments were used and each group was associated with a pair of counterclockwise/clockwise rotation angles (CCW/CW). In order to study only one variable at a time, one of the two angles was fixed and the second was increased or decreased. The distribution of angles was as follows: Group 1: 170°/60°; Group 2: 150°/60°; Group 3: 170°/30°; Group 4: 170°/90°; Group 5: 210°/60°. Thanks to a load/unload endodontic protocol carried out on a tensile bench, we quantified for each tested pair of angles (i) the cutting efficiency, (ii) the screwing effect and (iii) the generated torque.

RESULTS: Increasing or decreasing one of the two rotation angles influences the mechanical behavior of the instruments, as does the resulting range. Therefore, our results showed a direct influence of rotation angles on the mechanical behavior of endodontic instruments.

CONCLUSION: This study analyzes the influence of clockwise and counterclockwise rotation angles on the mechanical properties of 25/0.06 One Reciprocity instruments. The results of this work tend to demonstrate a direct influence of rotation angles on the mechanical behavior of 25/0.06 One Reciprocity instruments.

BDJ Open (2025)11:37; <https://doi.org/10.1038/s41405-025-00327-7>

INTRODUCTION

The latest endodontic major advancement is based on the mechanization of NiTi instruments in the mid-90s, the continuous rotation instrumental kinematic making the procedure safer and more reproducible [1–10]. More than 10 years after the arrival of continuous rotation, a new instrumental dynamic is shaking up the protocols of canal shaping. This new instrumental kinematic, called reciprocity, is an asymmetrical reciprocating movement involving an alternation of counterclockwise (CCW) and clockwise (CW) rotation angles. However, the reciprocating motion is more complex, involving a large number of parameters. In addition to the speed and rotation angles, other settings generally not communicated by the manufacturers, such as CCW and CW acceleration and deceleration, torque or standstill time at each change of direction, make these movements complex to analyze.

According to the scientific literature, this reciprocating motion offers several advantages such as the respect of canal trajectory [11], the elimination of debris as well as the reduction of dentinal microcracks [12]. This instrumental kinematic is especially advantageous to reduce cyclic fatigue and torsional stress [13, 14].

A large number of researches concerning the mechanical properties of instruments in terms of flexibility, cyclic fatigue,

resistance to torsion, and separation incidence have been carried out [15–32]. Heat treatment is one of the fundamental approaches used to modify the crystallographic arrangement of NiTi endodontic files [33–41], and thus their mechanical behaviors [42–47]. Many studies have compared endodontic files from different brands with various designs, kinematics, and heat treatment technologies [45–48]. All these studies showed mechanical improvement of heat treated endodontic files but highlight that many factors can influence mechanical resistance, each parameter influencing all the other ones. Therefore, for a fundamental approach, it seems important to test only one parameter at a time.

Among all these mechanical property researches, very few articles have directly focused on the influence of clockwise and counterclockwise rotation angles on the mechanical properties of reciprocity instruments. Reciprocity instruments generally have a left-handed pitch and their active angle, the largest, always goes in the pitch direction. Therefore, CCW angles give the instrument cutting efficiency, but also its screwing effects, while CW angles allow discharging the torsional stresses accumulated during cutting. The range between the two angles is also important and determines the ratio between cutting efficiency, screwing

¹Département de dentisterie restauratrice et endodontie, Faculté d'odontologie de Lorraine, Université de Lorraine, F-54000 Nancy, France. ²ERPI, Université de Lorraine, F-54000 Nancy, France. ³CNRS, IUL, Université de Lorraine, F-54000 Nancy, France. ⁴Faculté d'odontologie de Lorraine, Université de Lorraine, F-54000 Nancy, France. ⁵Faculté de médecine, EA 3450, Université de Lorraine, F-54000 Nancy, France. ⁶CNRS, LEM3, Université de Lorraine, F-57000 Metz, France. email: marin.vincent@univ-lorraine.fr

Received: 19 February 2025 Revised: 11 March 2025 Accepted: 11 March 2025

Published online: 12 April 2025

effect and discharge of torsional stresses. However, two reciprocity instruments can have a similar range, but different CCW and CW angles, leading to very different [49–53].

The present study aims to analyze the effect of different asymmetrical reciprocating rotation angles on the cutting efficiency and screwing effects of the One Recipro instrument (MicroMega, Besançon, France). The hypothesis of this study is that a single reciprocating setting could not be suitable for all clinical situations. A better understanding of this kinematic would certainly improve the conduct and reproducibility of endodontic treatments. In this perspective, several CCW and CW rotation angle pairs were evaluated during a load/unload endodontic protocol allowing for the recording of cutting efficiency and screwing effects, respectively. Simultaneously, the torque required for reciprocating motion was measured.

MATERIALS AND METHODS

Resin blocs

5 groups of 10 J shape resin blocks (Dentsply Sirona, Ballaigues, Switzerland) were employed for the performance and security tests. The used resin blocks present an average length of 18 mm, an apical permeability, and an average radius of curvature of 4.5 mm (Fig. 1). These endodontic blocks mimic challenging endodontic situations, according to the Endodontic Case Difficulty Assessment Form and Guidelines edited by the American Association of Endodontic.

Endodontic files

5 groups of 10 25/0.06 One Recipro instruments were used in this study. Table 1 shows the used endodontic protocol. Each group was associated with a pair of counterclockwise/clockwise rotation angles (CCW/CW). In order to study only one variable at a time, one of the two angles was fixe

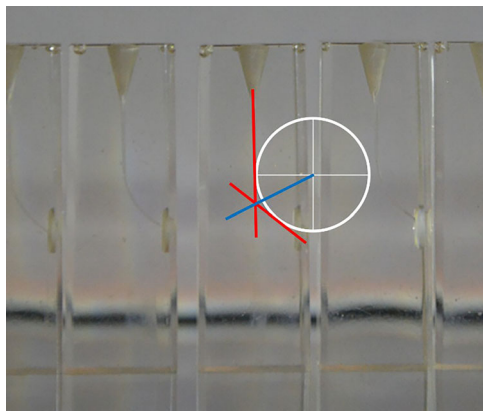


Fig. 1 The used endodontic resin blocks. The curvature angle and the radius of curvature are determined by the red and blue lines, respectively.

and the second was increased or decreased. All angle pairs are identified in CCW/CW direction. The distribution of angles was as follows: Group 1: 170°/60°; Group 2: 150°/60°; Group 3: 170°/30°; Group 4: 170°/90°; Group 5: 210°/60°.



Fig. 2 Tensile bench and endodontic assembly used for this study.

Table 1. Shaping protocol used for the endodontic tests.

Step	Instrument*	Working length	Kinematic parameters	Action
1	K. 10 file	18 mm		Root canal exploration + permeabilization
2	K.10 file	–	–	Permeabilization
3	One G instrument	18 mm	350 rpm 1.2 N.cm	Glide path
4	K.10 file	–	–	Permeabilization
5	Single use One RECI instrument	18 mm	170°/60° 150°/60° 170°/30° 170°/90° 210°/60°	Shaping
6	K.10 file	–	–	Permeabilization

Table 2. a Load/unload endodontic protocol: penetration level from 10 to 14 mm; b Load/unload endodontic protocol: penetration level from 14 to 16 mm; c Load/unload endodontic protocol: penetration level from 16 to 18 mm.

a						
			Penetration [mm]	Speed [mm/s]	Stop [s]	
Group 1	Cycle 1	Load	10	5		
		Unload	9.5	5		
	Cycle 2	Load	10.5	5		
		Unload	10	5		
	Cycle 3	Load	11	5		
		Unload	10.5	5		
Irrigation		−51	15	5		
Group 2	Cycle 4	Load	11.5	5		
		Unload	11	5		
	Cycle 5	Load	12	5		
		Unload	11.5	5		
	Cycle 6	Load	12.5	5		
		Unload	12	5		
Irrigation		−51	15	5		
Group 3	Cycle 7	Load	13	5		
		Unload	12.5	5		
	Cycle 8	Load	13.5	5		
		Unload	13	5		
	Cycle 9	Load	14	5		
		Unload	13.5	5		
Irrigation		−51	15	5		
b						
			Penetration [mm]	Speed [mm/s]	Stop [s]	
Group 4	Cycle 10	Load	14.25	2		
		Unload	14	2		
	Cycle 11	Load	14.5	2		
		Unload	14.25	2		
	Cycle 12	Load	14.75	2		
		Unload	14.5	2		
Group 5	Cycle 13	Load	15	2		
		Unload	14.75	2		
	Irrigation		−51	15		5
		Cycle 14	Load	15.25		2
	Unload		15	2		
	Group 6	Cycle 15	Load	15.5		2
Unload			15.25	2		
Cycle 16		Load	15.75	2		
		Unload	15.5	2		
Cycle 17		Load	16	2		
		Unload	15.75	2		
Irrigation		−51	15	5		
c						
			Penetration [mm]	Speed [mm/s]	Stop [s]	
Group 6	Cycle 18	Load	16.25	2		
		Unload	16	2		
	Cycle 19	Load	16.5	2		
		Unload	16.25	2		
Group 7	Irrigation		−51	15	5	
		Cycle 20	Load	16.75		2
	Unload		16.5	2		
	Cycle 21	Load	17	2		
Unload		16.75	2			
Irrigation		−51	15	5		

Table 2. continued

c			Penetration [mm]	Speed [mm/s]	Stop [s]
Group 8	Cycle 22	Load	17.25	2	
		Unload	17	2	
	Cycle 23	Load	17.5	2	
		Unload	17.25	2	
	Irrigation		−51	15	5
Group 9	Cycle 24	Load	17.75	2	
		Unload	17.5	2	
	Cycle 25	Load	18	2	
		Unload	17.75	2	
	Irrigation		−51	15	5

*irrigation with 96% ethanol irrigation is performed before and after each instrument pass to remove cutting debris.

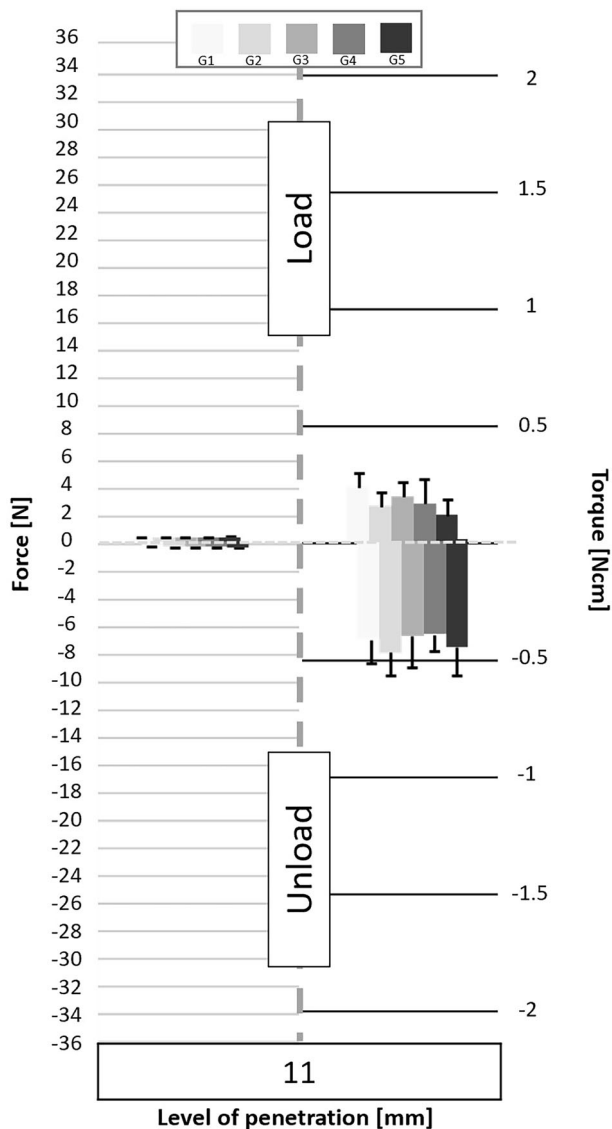


Fig. 3 Graphs of the forces and torque obtained during the load/unload endodontic tests at a penetration level of 11 mm.

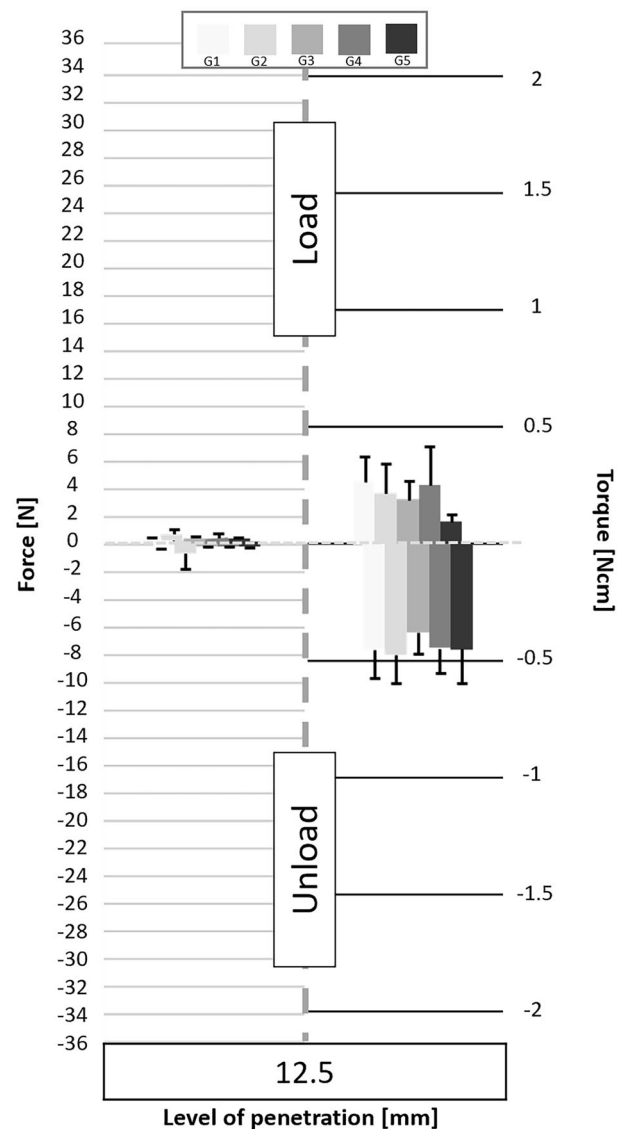


Fig. 4 Graphs of the forces and torque obtained during the load/unload endodontic tests at a penetration level of 12.5 mm.

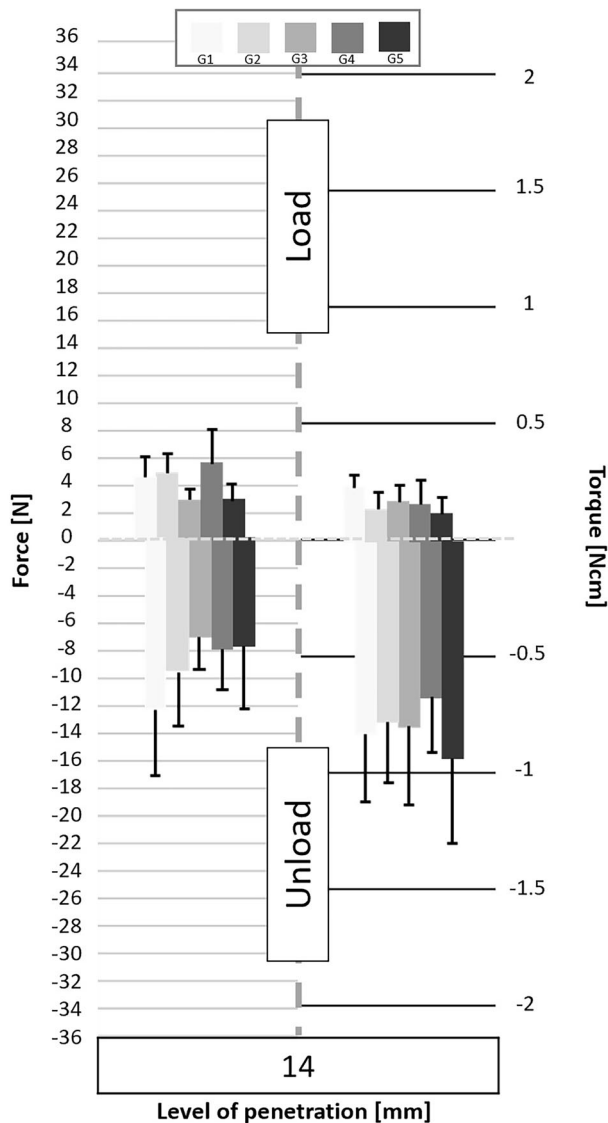


Fig. 5 Graphs of the forces and torque obtained during the load/unload endodontic tests at a penetration level of 14 mm.

All instruments were tested following a load/unload endodontic protocol. Before each test, the resin blocks were explored using a K.10 manual file for reproducibility purposes. In order to respect the clinical protocol of the One Recipro instruments, a glidepath with a 14/0.03 One G (MicroMega, Besançon, France) instrument was used before testing the One Recipro instruments.

Load/unload endodontic protocol

The load/unload endodontic protocol, allowing respectively downward/upward pecking motions, was carried out on a LS1 tensile bench (Ametek Lloyd Instruments Ltd., Bognor Regis, UK) controlled by the NexygenPlus software version 4.1.1.829 (Ametek, Berwyn, USA) in the dental engineering technical hall of the faculty of odontology of Lorraine (Campus Brabois Santé, University of Lorraine, France) (Fig. 2).

The tensile bench is composed of a platform on which the resin block is located. This platform is associated with a S2M/50N load cell with an output signal of 2 mV/V (HBM, Darmstadt, Germany) and a CS1211-B 0.3Nm torque sensor (TE Connectivity Measurement Specialties, Galway, Ireland). The endodontic instrument is inserted on an endodontic contra-angle connected to a programmable endodontic motor (Dual Move®, Micro-Mega, Besançon, France). The endodontic motor is connected to the column and carries out the up-and-down pecking motions required by the protocol. Thanks to the micrometric screws, the axis of the tested endodontic instrument can be perfectly aligned with that of the resin

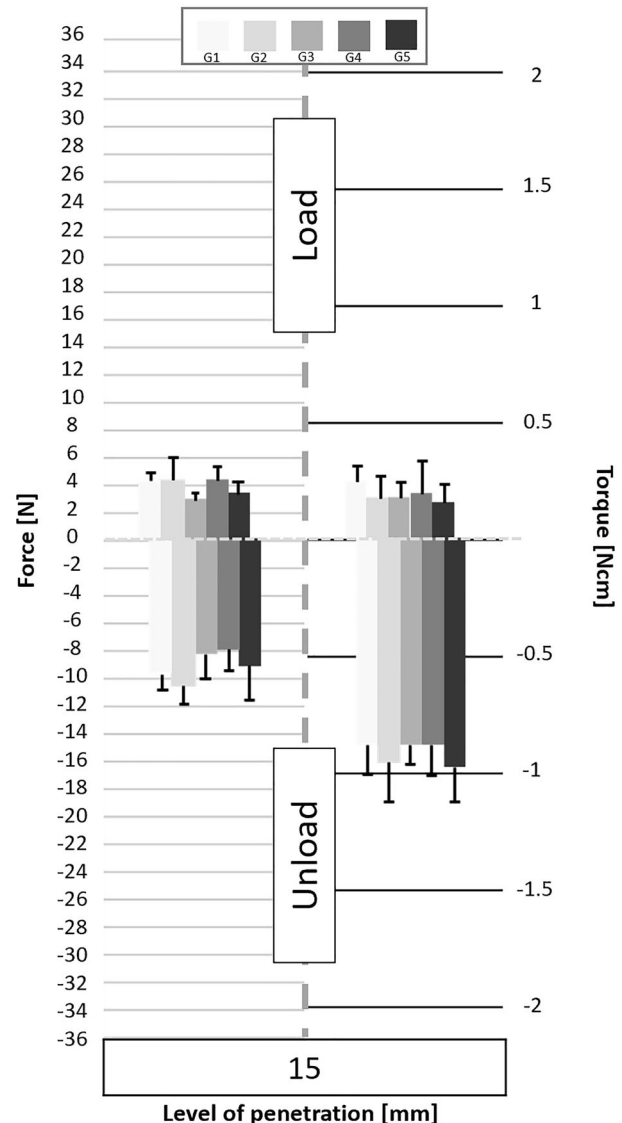


Fig. 6 Graphs of the forces and torque obtained during the load/unload endodontic tests at a penetration level of 15 mm.

block canal. The instrument under test is positioned from the occlusal edge of the resin block using an automatic detection tool.

The protocol corresponds to a free load/unload test involving 25 successive cycles, divided into 9 groups of cycles, allowing the up-and-down pecking motion of the tested endodontic instrument in a resin block [54]. The instrumental pressure was kept constant and reproducible thanks to our experimental protocol obtained by the association of (i) a constant up-and-down pecking speed controlled by the bench, (ii) a constant instrumental kinematics given by the same endodontic motor and (iii) a machining of the same resin blocks with (iv) the same instruments. Therefore, this protocol made it possible to directly analyze the instrumental cutting efficiency and screwing effects. Changing a parameter, here the rotation angles and thus the instrumental kinematics, allows testing its influence on the instrumental cutting efficiency and screwing effects during the shaping of the resin block.

Complete instrumental withdrawal is performed between each cycle allowing (i) a canal irrigation with 1 mL of 96% ethanol to remove debris and (ii) a verification of the apical patency. This protocol was established to be reproducible. To mimic the clinical reality, three groups of parameters appropriate to the work of the associated canal section were determined as follows:

- Canal penetration from 10 to 14 mm, before the curvature (Table 2a),
- Canal penetration from 14 to 16 mm, in the coronal part of the curvature (Table 2b),

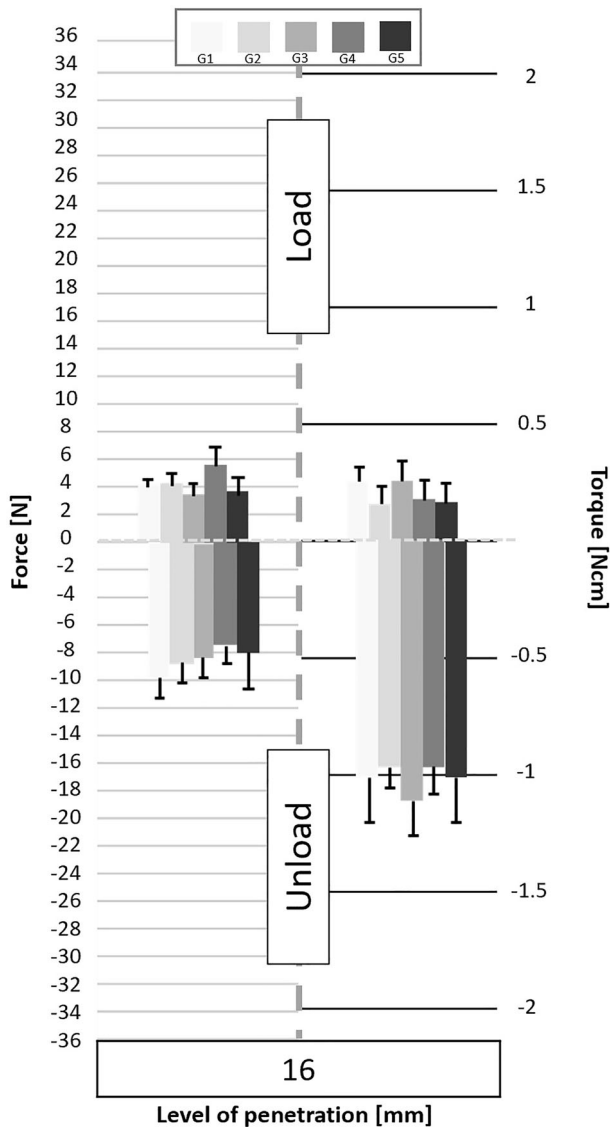


Fig. 7 Graphs of the forces and torque obtained during the load/unload endodontic tests at a penetration level of 16 mm.

- Canal penetration from 16 to 18 mm, in the apical part of the curvature (Table 2c).

The torque, the vertical components of the force and displacement are recorded at a rate of 26 Hz. At the end of each test, the maximum load and unload values are recorded for each group of cycles.

Statistics

Numerical data were analyzed using non-parametric Kruskal-Wallis statistical tests with Dunn's correction ($\alpha = 0.05$) for multiple comparisons. The results were considered statistically significant for a P value < 0.05 . All statistical analyzes were performed using GraphPad Prism® software (San Diego, California, US).

RESULTS

Following the processing of the data collected by the cell force, the minimum and maximum values of cycles were analyzed. Figures 3 to 11 show the load/unload forces and the associated load/unload torque of the different tested pairs of angles in function of the penetration level. The data on the graph are presented with means \pm standard deviations. Results are presented in Tables 3a to 4b and

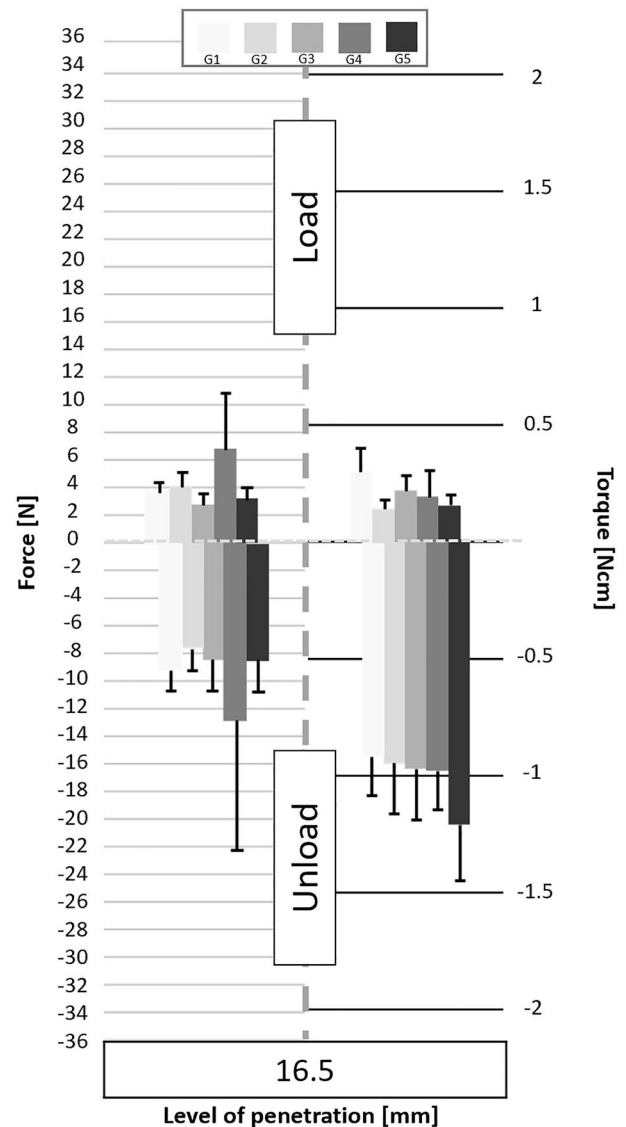


Fig. 8 Graphs of the forces and torque obtained during the load/unload endodontic tests at a penetration level of 16.5 mm.

detail respectively (i) the differences in the load/unload forces and (ii) the differences in the associated load/unload torque of the different pairs of rotation angles.

Loading time

The positive forces obtained during the downward pecking motions, corresponding to the loading times, essentially underline the cutting effect of the instruments. Several significant differences are found (Table 3a). The analysis of the load force results shows that:

- the G3 group obtains the best results;
- the G4 group obtains the worst results;
- groups G1, G2 and G5 do not highlight any significant differences; however, the results give the following trend: $G5 > G1 > G2$.

Torque represents the energy required by the endodontic motor to maintain a constant rotation speed regardless of the encountered constraint. During the loading times, the analysis of the torque results does not show any real difference (Table 3b). Nevertheless, group G5 obtains the lowest load torque values.

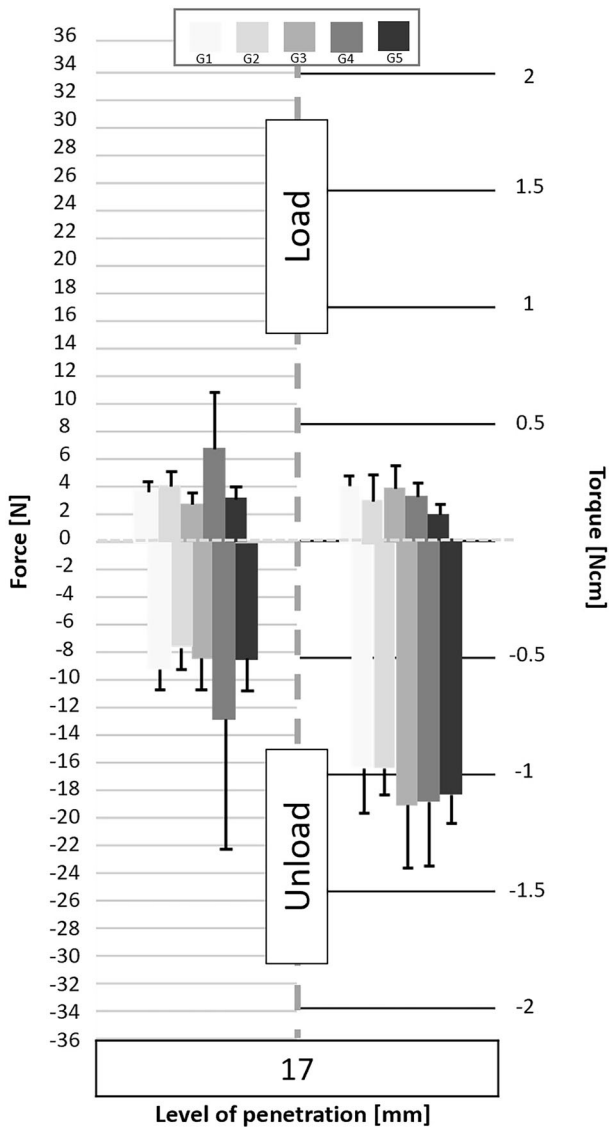


Fig. 9 Graphs of the forces and torque obtained during the load/unload endodontic tests at a penetration level of 17 mm.

Therefore, it seems that:

- for a same CCW angle, a reduction in the CW angle improves the cutting efficiency (G3 is the best group);
- for a same CCW angle, an increase in the CW angle reduces the cutting efficiency (G4 is the worst group);
- the greater the difference between the two angles, the greater the cutting efficiency (G5 > G1 > G2);
- the greater the difference between the two angles, the lower the load torque (G5 > G2).

Unloading times

The negative forces obtained during the upward pecking motions, corresponding to the unloading times, essentially highlight the screwing effects which oppose the withdrawal of the instrument. Some significant differences are found (Table 4a). The analysis of the unload force results shows that:

- the G4 group obtains the worst results in the apical region;
- the groups G1, G2, G3 and G5 do not highlight any significant

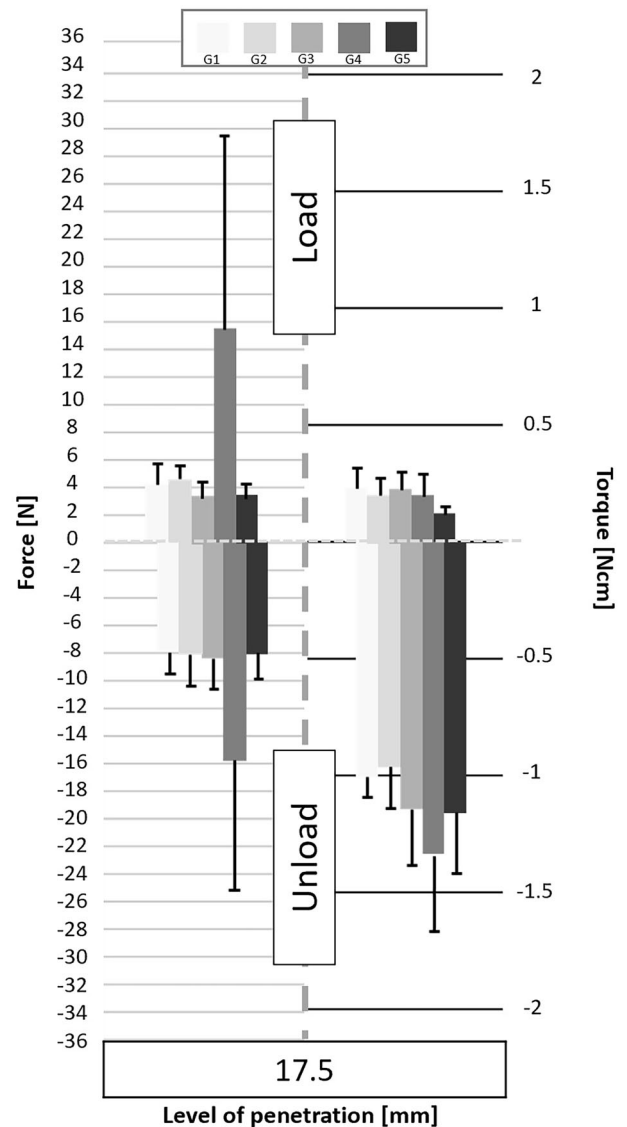


Fig. 10 Graphs of the forces and torque obtained during the load/unload endodontic tests at a penetration level of 17.5 mm.

differences except at 14 mm and 15 mm where G1 and G2 are significantly worst; however, the results give the following trend: G5 > G1, G2, G3, G4.

During the unload times, the analysis of the torque results does not show any difference (Table 4b). The trends are:

- groups G1 and G2 obtain the lowest unload torque values;
- group G4 obtains the highest unload torque values in the last millimeter.

Therefore, it seems that:

- for the same CCW angle, an increase in the CW angle increases the screwing effect during maximum sheathing (G4 is the worst group);
- for the same CW angle, a reducing in the CCW cutting angle increases the screwing effect at the beginning of the curvature (G1 et G2 are the worst groups);
- for the same CW angle, an increase of range between the two angles linked to a strong increase of the CCW angle seems to slightly reduce the screwing effect (G5);

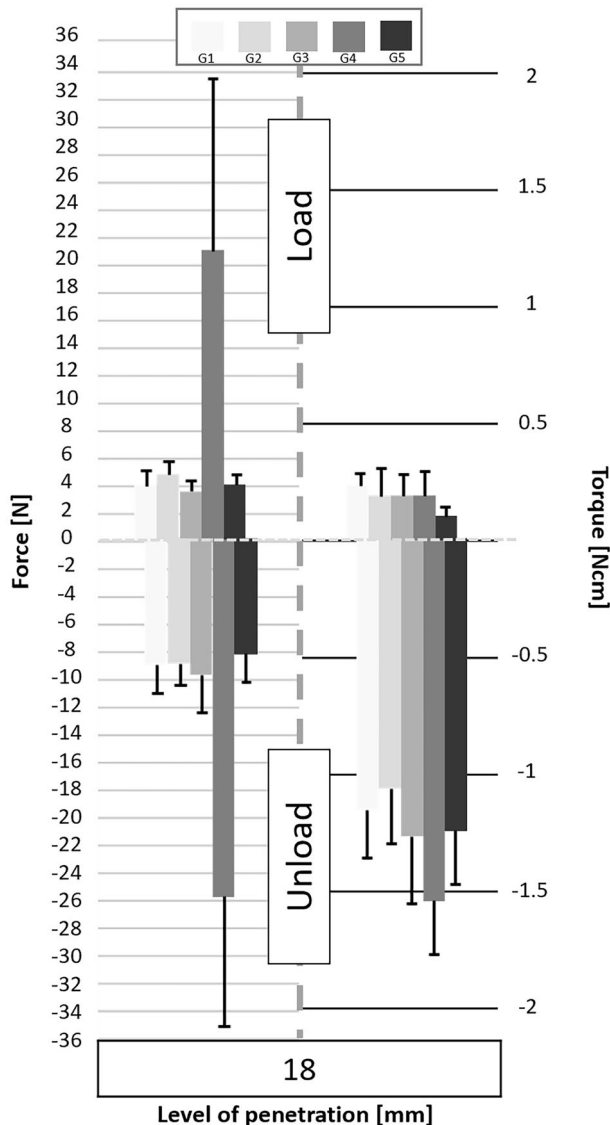


Fig. 11 Graphs of the forces and torque obtained during the load/unload endodontic tests at a penetration level of 18 mm.

- for the same CW angle, an increase of the CCW angle increases the unload torque (G5 is the worst group).

DISCUSSION

While the literature describes resistance to cyclic fatigue and resistance to torsion as advantages of the reciprocating motion, apical debris extrusion or canal transportation, for example, seem to be more questionable [12]. These differences in conclusions are related to the complexity of analyzing the kinematics of the asymmetrical reciprocating motion [55, 56]. Each reciprocity instrument is only qualified for a given pair of angles and a given rotational speed, leaving the practitioner free to use it on the endodontic motor of its choice. Nevertheless, other settings, especially CCW and CW acceleration and deceleration, torque or standstill time at each change of direction, are generally not communicated nor configurable. These settings are directly linked to the ability of endodontic motors to be reproducible between them, while the literature highlights the opposite [57–59]. Therefore, in addition to its complex settings, this kinematic is

dependent on the power of the rotating motor and their clinical usage [57, 60, 61]. All these reasons could explain the disparities found on the asymmetrical reciprocating motion kinematics in the literature, underlining the need for an evidence-based approach.

The aim of our study was to analyze the influence of the CCW/CW rotation angles on the mechanical behavior of the One Reciprocity instrument. For this purpose, we quantified for each tested pair of angles (i) the cutting efficiency linked to the load forces, (ii) the screwing effect linked to the unload forces and (iii) the torque linked to the ability of the endodontic motor to maintain a constant rotation speed.

Based on the obtained load forces, we can classify the tested pair of angles as follows:

$170^\circ/30^\circ$ (G3) > $210^\circ/60^\circ$ (G5) > $170^\circ/60^\circ$ (G1) > $150^\circ/60^\circ$ (G2) > $170^\circ/90^\circ$ (G4)

Load forces, linked to the cutting efficiency, increase as the instrument advances into the canal. However, load associated torques remain relatively stable throughout the preparation. Angle variations do not affect the load torque required to the progression of the instrument into the canal. Increasing the clockwise angles decreases the cutting capacity of the instrument, especially in the last apical millimeter when the instrument encounters high resistance (G4), while decreasing them increases the cutting capacity (G3) due to a higher number of rotation cycles per minute. The most important parameter is the difference between the two angles: the greater the range, the more effective the cut (G5). Nevertheless, according to Saber and al. (2013), the reduction of the reciprocity range will increase resistance to cyclic fatigue, allow better centering, decrease canal transport, but increase preparation [49]. Others studies confirmed that reducing the range of reciprocity, by decreasing the CCW angle, improves resistance to cyclic fatigue [50, 51]. Therefore, a high range linked to a high CCW rotation angle would improve the performance of the instrument, but would reduce the safety of use.

Based on the obtained unload forces, we can classify the tested pair of angles as follows:

$210^\circ/60^\circ$ (G5) > $170^\circ/60^\circ$ (G1) > $150^\circ/60^\circ$ (G2) > $170^\circ/30^\circ$ (G3) > $170^\circ/90^\circ$ (G4)

Increasing the clockwise angles increases the unload forces linked to screwing effects (G4), while an increase in the CCW angle decreases them (G5). Experimental conditions with a constant descent speed of the instrument in the canal, combined with the high CW angle (G4), do not allow for sufficiently rapid shaping of the canal, which promote tip binding. As a result, the unload forces required for its disengagement are increased Omori et al. [53]. compared the effect caused by an increase in the range of reciprocity between the angles $150^\circ/30^\circ$ and $240^\circ/120^\circ$ [53]. They found that the instrument with $240^\circ/120^\circ$ angles showed fewer screwing forces compared to its homologue with $150^\circ/30^\circ$ angles. Therefore, it would have been interesting to test an increase in overall range by increasing both the CW and CCW angles to validate these results with the One Reciprocity instrument. Our results show that an increase of range linked to a CCW angle increase (G5) tend to decrease the screwing effects. Also, it would be interesting to validate this hypothesis during an increase in range linked to a decrease in CW angle.

Regarding torque, the load values are generally consistent regardless of the CCW/CW angle pairs and penetration levels. This could be explained by our experimental conditions, which involved only a same type of instrument, a same canal geometry, and a same load speed setting. However, the high 210° CCW angle of G5, providing better cutting efficiency and easier progression within the canal, could potentially explain its lower load torque values.

For the same reasons related to the experimental conditions, the consistency of torque values during unload can also be observed. However, the values obtained for group G4 in the last apical millimeter could be explained by its high 90° CW angle, causing tip binding and thus requiring higher unload torque to maintain

Table 3. a Positive forces obtained during the downward pecking motion. The significant differences are in favor of the groups noted in the column; b Torques obtained during the downward pecking motions. The significant differences are in favor of the groups noted in the column.

a		b	
Penetration [mm]		Penetration [mm]	
Significance		Significance	
11		11	
12.5		12.5	
14		14	
15		15	
16		16	
16.5		16.5	
17		17	
17.5		17.5	
18		18	
11		11	
12.5		12.5	
14		14	
15		15	
16		16	
16.5		16.5	
17		17	
17.5		17.5	
18		18	
11		11	
12.5		12.5	
14		14	
15		15	
16		16	
16.5		16.5	
17		17	
17.5		17.5	
18		18	
11		11	
12.5		12.5	
14		14	
15		15	
16		16	
16.5		16.5	
17		17	
17.5		17.5	
18		18	
11		11	
12.5		12.5	
14		14	
15		15	
16		16	
16.5		16.5	
17		17	
17.5		17.5	
18		18	
11		11	
12.5		12.5	
14		14	
15		15	
16		16	
16.5		16.5	
17		17	
17.5		17.5	
18		18	
11		11	
12.5		12.5	
14		14	
15		15	
16		16	
16.5		16.5	
17		17	
17.5		17.5	
18		18	
11		11	
12.5		12.5	
14		14	
15		15	
16		16	
16.5		16.5	
17		17	
17.5		17.5	
18		18	
11		11	
12.5		12.5	
14		14	
15		15	
16		16	
16.5		16.5	
17		17	
17.5		17.5	
18		18	
11		11	
12.5		12.5	
14		14	
15		15	
16		16	
16.5		16.5	
17		17	
17.5		17.5	
18		18	
11		11	
12.5		12.5	
14		14	
15		15	
16		16	
16.5		16.5	
17		17	
17.5		17.5	
18		18	
11		11	
12.5		12.5	
14		14	
15		15	
16		16	
16.5		16.5	
17		17	
17.5		17.5	
18		18	
11		11	
12.5		12.5	
14		14	
15		15	
16		16	
16.5		16.5	
17		17	
17.5		17.5	
18		18	
11		11	
12.5		12.5	
14		14	
15		15	
16		16	
16.5		16.5	
17		17	
17.5		17.5	
18		18	
11		11	
12.5		12.5	
14		14	
15		15	
16		16	
16.5		16.5	
17		17	

Group 1: 170°/60°; Group 2: 150°/60°; Group 3: 170°/30°; Group 4: 170°/90°; Group 5: 210°/60°. * $P < 0.05$; ** $P < 0.01$; *** $P < 0.001$; **** $P < 0.0001$.

rotation speed during disengagement. G1 and G2 achieve the best lowest unload torque values: the lower the range linked to a low CCW rotation angle, the lower the unload torque values. It would be interesting to observe if the same results would be obtained for a decrease of range linked to the CW angle.

All of these potential mechanical behavior improvements are achieved by forcing the endodontic motor into a configuration for which the One Reci instrument has not been qualified. To exploit all these data at once, it would be necessary to implement these scenarios in endodontic motors monitoring in real time the pressure forces and the torque undergone by the instrument to identify the best pair of angle configuration according to the clinical situations. Effectively, literature has shown that motors capable of adapting the kinematic of endodontic instruments according to the perceived constraints by the instruments make it possible to improve their mechanical behaviors. Thanks to this monitoring, the endodontic motor will adapt its movement to each clinical situation and improve the safety of endodontic treatment [61, 62].

With a fundamental approach, the main objective of our collection method was to change only one variable at a time and to fix all the other parameters. The use of a tensile bench made it possible to maintain a constant instrumental pressure through (i) a constant up-and-down pecking speed, (ii) the use of a single endodontic motor, (iii) a single type of endodontic simulator and (iv) a single type of instrument. This constant pressure allows the reproducible analyze of the instrumental cutting efficiency and screwing effects. Therefore, any modification of the instrumental settings allow to directly analyze its impact on these two mechanical behaviors. The fully automated and computerized

system ensured the reproducibility of the data collection. Likewise, because the measured endodontic motors values differ from the manufacturers' declared values [55, 56], the association of a torque sensor to the tensile bench allows reproducibility of torque data regardless of the tested motor. Another study highlights that these experimental conditions can be adapted to different motors and different kinematics [61]. However, we emphasize human intervention during the time of irrigation and verification of the apical patency. Therefore, a fully automated solution could make it possible to propose a reproducible method allowing an evidence-based approach in terms of cutting efficiency and screwing effects.

Finally, further studies are needed to extend these results to other endodontic reciprocating instruments. In addition, tests on extracted natural teeth could validate the obtained preclinical results. Indeed, the use of resin blocks allows better experimental standardization, but their mechanical properties differ from those of dental tissues [63].

CONCLUSION

Within the limits of our study, the best way to increase the performance of the One Reciprocal instrument seems to be:

- to reduce the CW rotation angle, thus promote the active movement, when high cutting efficiency is desired (G3);
- to increase the range linked to a high CCW rotation angle when a compromise between cutting effective, screwing effect and torque is desired (G5);
- to avoid an increase of CW rotation angle to prevent screwing effects and unload torque increases (G4);

Table 4. a Negative forces obtained during the upward pecking motions. The significant differences are in favor of the groups noted in the column; b Torques obtained during the upward pecking motions. The significant differences are in favor of the groups noted in the column.

a		Group 1	Group 2	Group 3	Group 4	Group 5
Penetration [mm]		11 12.5 14 15 16 16.5 17 17.5 18	11 12.5 14 15 16 16.5 17 17.5 18	11 12.5 14 15 16 16.5 17 17.5 18	11 12.5 14 15 16 16.5 17 17.5 18	11 12.5 14 15 16 16.5 17 17.5 18
Significativity		(4) *	(4) (4) *	(1) (2) *	(2) *	(4) *

b		Group 1	Group 2	Group 3	Group 4	Group 5
Penetration [mm]		11 12.5 14 15 16 16.5 17 17.5 18	11 12.5 14 15 16 16.5 17 17.5 18	11 12.5 14 15 16 16.5 17 17.5 18	11 12.5 14 15 16 16.5 17 17.5 18	11 12.5 14 15 16 16.5 17 17.5 18
Significativity		(5) *	(4) *	(4) (4) *		

Group 1: 170°/60°; Group 2: 150°/60°; Group 3: 170°/30°; Group 4: 170°/90°; Group 5: 210°/60°. * $P < 0.05$; ** $P < 0.01$; *** $P < 0.001$; **** $P < 0.0001$.

- to reduce the range linked to a low CCW rotation angle when a low unload torque is desired (G1 and G2).

Therefore, our results allow to conclude on a direct influence of rotation angles on the mechanical behavior of endodontic instruments. The implementation of these data could improve the mechanical behavior of reciprocating instruments. Endodontic motors monitoring torque and pressure in real time could be a solution to adapt kinematic and mechanical behavior of instruments according to the different encountered clinical situations.

DATA AVAILABILITY

The data that support the findings of this study are available from the corresponding author upon reasonable request.

REFERENCES

- Cheung GSP, Liu CSY. A retrospective study of endodontic treatment outcome between nickel-titanium rotary and stainless steel hand filing techniques. *J Endod.* 2009;35:938–43.
- Esposito PT, Cunningham CJ. A comparison of canal preparation with nickel-titanium and stainless steel instruments. *J Endod.* 1995;21:173–6.
- Glossen CR, Haller RH, Dove SB, del Rio CE. A comparison of root canal preparations using Ni-Ti hand, Ni-Ti engine-driven, and K-Flex endodontic instruments. *J Endod.* 1995;21:146–51.
- Kazemi RB, Stenman E, Spångberg LS. A comparison of stainless steel and nickel-titanium H-type instruments of identical design: torsional and bending tests. *Oral Surg Oral Med Oral Pathol Oral Radio Endod.* 2000;90:500–6.
- Samyn JA, Nicholls JL, Steiner JC. Comparison of stainless steel and nickel-titanium instruments in molar root canal preparation. *J Endod.* 1996;22:177–81.
- Saunders E. Hand instrumentation in root canal preparation. *Endod Top.* 2005;10:163–7.
- Schrader C, Ackermann M, Barbakow F. Step-by-step description of a rotary root canal preparation technique. *Int Endod J.* 1999;32:312–20.
- Short JA, Morgan LA, Baumgartner JC. A comparison of canal centering ability of four instrumentation techniques. *J Endod.* 1997;23:503–7.
- Thompson SA. An overview of nickel-titanium alloys used in dentistry. *Int Endod J.* 2000;33:297–310.
- Walia HM, Brantley WA, Gerstein H. An initial investigation of the bending and torsional properties of Nitinol root canal files. *J Endod.* 1988;14:346–51.
- Giuliani V, Di Nasso L, Pace R, Pagavino G. Shaping ability of waveone primary reciprocating files and ProTaper system used in continuous and reciprocating motion. *J Endod.* 2014;40:1468–71.
- Ahn SY, Kim HC, Kim E. Kinematic effects of Nickel-titanium instruments with reciprocating or continuous rotation motion: a systematic review of in vitro studies. *J Endod.* 2016;42:1009–17.
- Sekar V, Kumar R, Nandini S, Ballal S, Velmurugan N. Assessment of the role of cross section on fatigue resistance of rotary files when used in reciprocation. *Eur J Dent.* 2016;10:541–5.
- Pérez-Higueras JJ, Arias A, de la Macorra JC. Cyclic fatigue resistance of K3, K3XF, and twisted file nickel-titanium files under continuous rotation or reciprocating motion. *J Endod.* 2013;39:1585–8.
- Ahmad MZ, Sadaf D, MacBain MM, Merdad KA. Effect of mode of rotation on apical extrusion of debris with four different single-file endodontic instrumentation systems: Systematic review and meta-analysis. *Aust Endod J.* 2022;48:202–18.
- Ruddle CJ. Nickel-titanium rotary systems: review of existing instruments and geometries. *Dent Today.* 2000;19:90–5.
- Akhlaghi NM, Dadresanfar B, Darmiani S, Moshari A. Effect of master apical file size and taper on irrigation and cleaning of the apical third of curved canals. *J Dent Tehran Univ Med Sci.* 2014;11:188–95.
- Capar ID, Arslan H, Akcay M, Ertas H. An in vitro comparison of apically extruded debris and instrumentation times with ProTaper Universal, ProTaper Next, Twisted File Adaptive, and HyFlex instruments. *J Endod.* 2014;40:1638–41.
- Kim HC, Kim HJ, Lee CJ, Kim BM, Park JK, Versluis A. Mechanical response of nickel-titanium instruments with different cross-sectional designs during shaping of simulated curved canals. *Int Endod J.* 2009;42:593–602.
- Schäfer E, Tepel J. Relationship between design features of endodontic instruments and their properties. Part 3. Resistance to bending and fracture. *J Endod.* 2001;27:299–303.
- Dablanca-Blanco AB, Castelo-Baz P, Miguéns-Vila R, Álvarez-Novoa P, Martín-Biedma B. Endodontic Rotary Files, What Should an Endodontist Know?. *Med Kaunas Lith.* 2022;58:719.
- Ferraz CC, Gomes NV, Gomes BP, Zaia AA, Teixeira FB, Souza-Filho FJ. Apical extrusion of debris and irrigants using two hand and three engine-driven instrumentation techniques. *Int Endod J.* 2001;34:354–8.
- Yared G. Canal preparation using only one Ni-Ti rotary instrument: preliminary observations. *Int Endod J.* 2008;41:339–44.

24. Schäfer E, Schulz-Bongert U, Tulus G. Comparison of hand stainless steel and nickel titanium rotary instrumentation: a clinical study. *J Endod.* 2004;30:432–5.
25. Pedullà E, Grande NM, Plotino G, Gambarini G, Rapisarda E. Influence of continuous or reciprocating motion on cyclic fatigue resistance of 4 different nickel-titanium rotary instruments. *J Endod.* 2013;39:258–61.
26. Orhan EO, Bahadır D, Irmak O. Kinematics of « adaptive motion » under constant torque values. *J Endod.* 2022;48:355–61.
27. Ferreira F, Adeodato C, Barbosa I, Aboud L, Scelza P, Zaccaro Scelza M. Movement kinematics and cyclic fatigue of NiTi rotary instruments: a systematic review. *Int Endod J.* 2017;50:143–52.
28. Çapar ID, Arslan H. A review of instrumentation kinematics of engine-driven nickel-titanium instruments. *Int Endod J.* 2016;49:119–35.
29. Pedrinha VF, Brandão JMDS, Pessoa OF, Rodrigues PA. Influence of file motion on shaping, apical debris extrusion and dentinal defects: a critical review. *Open Dent J.* 2018;12:189–201.
30. Anderson ME, Price JWH, Parashos P. Fracture resistance of electropolished rotary nickel-titanium endodontic instruments. *J Endod.* 2007;33:1212–6.
31. Rapisarda E, Bonaccorso A, Tripi TR, Fragalk I, Condorelli GG. The effect of surface treatments of nickel-titanium files on wear and cutting efficiency. *Oral Surg Oral Med Oral Pathol Oral Radio Endod.* 2000;89:363–8.
32. Boessler C, Paque F, Peters OA. The effect of electropolishing on torque and force during simulated root canal preparation with ProTaper shaping files. *J Endod.* 2009;35:102–6.
33. Shen Y, Zhou HM, Wang Z, Campbell L, Zheng YF, Haapasalo M. Phase transformation behavior and mechanical properties of thermomechanically treated K3XF nickel-titanium instruments. *J Endod.* 2013;39:919–23.
34. Plotino G, Testarelli L, Al-Sudani D, Pongione G, Grande NM, Gambarini G. Fatigue resistance of rotary instruments manufactured using different nickel-titanium alloys: a comparative study. *Odontology.* 2014;102:31–5.
35. Kuhn G, Jordan L. Fatigue and mechanical properties of nickel-titanium endodontic instruments. *J Endod.* 2002;28:716–20.
36. Hayashi Y, Yoneyama T, Yahata Y, Miyai K, Doi H, Hanawa T, et al. Phase transformation behaviour and bending properties of hybrid nickel-titanium rotary endodontic instruments. *Int Endod J.* 2007;40:247–53.
37. Johnson E, Lloyd A, Kuttler S, Namerow K. Comparison between a novel nickel-titanium alloy and 508 nitinol on the cyclic fatigue life of ProFile 25/04 rotary instruments. *J Endod.* 2008;34:1406–9.
38. Zanza A, Seracchiani M, Reda R, Di Nardo D, Gambarini G, Testarelli L. Role of the Crystallographic Phase of NiTi rotary instruments in determining their torsional resistance during different bending conditions. *Mater Basel Switz.* 2021;14:6324.
39. Abdelmomen I, Vincent M, Thiebaud F, Budzinski J, Bastogne T, Ben Zineb T, et al. Experimental Analysis of the Influence of Heat Treatments on the Flexibility of NiTi Alloy for Endodontic Instruments Manufacturing. *Mater Basel Switz.* 2023;16:3437.
40. Shen Y, Zhou HM, Zheng YF, Peng B, Haapasalo M. Current challenges and concepts of the thermomechanical treatment of nickel-titanium instruments. *J Endod.* 2013;39:163–72.
41. Choi J, Oh S, Kim YC, Jee KK, Kum K, Chang S. Fracture resistance of K3 Nickel-titanium files made from different thermal treatments. *Bioinorg Chem Appl.* 2016;2016. 6374721.
42. De-Deus G, Silva EJNL, Vieira VTL, Belladonna FG, Elias CN, Plotino G, et al. Blue thermomechanical treatment optimizes fatigue resistance and flexibility of the reciproc files. *J Endod.* 2017;43:462–6.
43. Hamdy TM, Galal M, Ismail AG, Abdelraouf RM. Evaluation of flexibility, micro-structure and elemental analysis of some contemporary nickel-titanium rotary instruments. *Open Access Maced J Med Sci.* 2019;7:3647–54.
44. Goo HJ, Kwak SW, Ha JH, Pedullà E, Kim HC. Mechanical Properties of Various Heat-treated Nickel-titanium Rotary Instruments. *J Endod.* 2017;43:1872–7.
45. Özyürek T, Gündoğar M, Yılmaz K, Uslu G. Bending resistance and cyclic fatigue life of Reciproc Blue, WaveOne Gold, and Genius files in a double (S-shaped) curved canal. *J Dent Res Dent Clin Dent Prospects.* 2017;11:241–6.
46. Oh S, Kum KY, Cho K, Lee SH, You SH, Go J, et al. Torsional and bending properties of V Taper 2H, ProTaper NEXT, NRT, and one shape. *BioMed Res Int.* 2019;2019:6368958.
47. Oh S, Kum KY, Kim HJ, Moon SY, Kim HC, Chaniotis A, et al. Bending resistance and cyclic fatigue resistance of WaveOne Gold, Reciproc Blue, and HyFlex EDM instruments. *J Dent Sci.* 2020;15:472–8.
48. Seracchiani M, Miccoli G, Reda R, Zanza A, Vanlenti Obino F, Bhandi S, et al. A Comprehensive in vitro comparison of mechanical properties of two rotary endodontic instruments. *World J Dent.* 2020;11:185–8.
49. Saber SEDM, Abu El Sadat SM. Effect of altering the reciprocation range on the fatigue life and the shaping ability of WaveOne nickel-titanium instruments. *J Endod.* 2013;39:685–8.
50. Gambarini G, Rubini AG, Al Sudani D, Gergi R, Culla A, De Angelis F, et al. Influence of different angles of reciprocation on the cyclic fatigue of nickel-titanium endodontic instruments. *J Endod.* 2012;38:1408–11.
51. Shin CS, Huang YH, Chi CW, Lin CP. Fatigue life enhancement of NiTi rotary endodontic instruments by progressive reciprocating operation. *Int Endod J.* 2014;47:882–8.
52. Al-Sudani D, Kaabi H, Al Gamdi A, Al Dakheel A. The influence of different angles and reciprocation on the shaping ability of two nickel-titanium rotary root canal instruments. *J Contemp Dent Pr.* 2014;15:451–5.
53. Omori S, Ebihara A, Hirano K, Kasuga Y, Unno H, Nakatsukasa T, et al. Effect of Rotational Modes on Torque/Force Generation and Canal Centering Ability during Rotary Root Canal Instrumentation with Differently Heat-Treated Nickel-Titanium Instruments. *Mater Basel Switz.* 2022;15:6850.
54. Vincent M, Xolin P, Gevrey AM, Thiebaud F, Engels-Deutsch M, Ben Zineb T. Experimental and numerical analysis of penetration/removal response of endodontic instrument made of single crystal Cu-based SMA: comparison with NiTi SMA instruments. *Smart Mater Struct.* 2017;26:045014.
55. Fidler A. Kinematics of 2 reciprocating endodontic motors: the difference between actual and set values. *J Endod.* 2014;40:990–4.
56. Fidler A, Orhan E, Irmak O. Computer-aided phase identification and frame-to-frame analysis of endodontic asymmetric reciprocation rotation: a preliminary study. *Image Anal Stereo.* 2020;39:91–9.
57. Irmak Ö, Orhan EO. Kinematic analysis of new and used reciprocating endodontic motors in 2 different modes. *Int J Artif Organs.* 2017;0.
58. Braambati D, Monteiro Netto RC, Coelho MS, Soares AJ, Frozoni M. Reciprocating kinematics of X-Smart Plus, VDW silver and, iroot endodontic motors: a comparison between real and set values. *Braz Dent J.* 2022;33:28–35.
59. Monteiro-Netto RC, Braambati D, Arruda-Vasconcelos R, Soares AD, Frozoni M. Evaluation of the rotary kinematics between actual and set speeds of X-Smart Plus, VDW Silver and iRoot motors. *Braz Dent J.* 2023;34:21–6.
60. Orhan EO, Irmak O, Ertugrul IF. Kinematics of a novel reciprocating endodontic handpiece. *Int Endod J.* 2019;52:1235–43.
61. Reynette C, Giess R, Davril J, Martrette JM, Mortier É, Balthazard R, et al. Influence of endodontic motors on the behaviour of root canal shaping instruments: an in vitro comparative study. *BDJ Open.* 2023;9:51.
62. Gambarini G. Rationale for the use of low-torque endodontic motors in root canal instrumentation. *Endod Dent Traumatol.* 2000;16:95–100.
63. Weine FS, Kelly RF, Lio PJ. The effect of preparation procedures on original canal shape and on apical foramen shape. *J Endod.* 1975;1:255–62.

AUTHOR CONTRIBUTIONS

Corresponding author: MV; Conceptualization: MV; Methodology: RG; MD; MV; Formal analysis: MV; RG; Investigation: RG; MD; RH; MV; Data curation: RB; Writing—original draft preparation: RG; EM; MV; Writing—review and editing: RG; EM; MD; RH; J-MM; RB; MV; Visualization: RG; EM; MV; Supervision: RH; EM; MV; Project administration: MV. All authors have read and agreed to the published version of the manuscript.

COMPETING INTERESTS

The authors declare no competing interests.

ADDITIONAL INFORMATION

Correspondence and requests for materials should be addressed to Marin Vincent.

Reprints and permission information is available at <http://www.nature.com/reprints>

Publisher's note Springer Nature remains neutral with regard to jurisdictional claims in published maps and institutional affiliations.



Open Access This article is licensed under a Creative Commons Attribution 4.0 International License, which permits use, sharing, adaptation, distribution and reproduction in any medium or format, as long as you give appropriate credit to the original author(s) and the source, provide a link to the Creative Commons licence, and indicate if changes were made. The images or other third party material in this article are included in the article's Creative Commons licence, unless indicated otherwise in a credit line to the material. If material is not included in the article's Creative Commons licence and your intended use is not permitted by statutory regulation or exceeds the permitted use, you will need to obtain permission directly from the copyright holder. To view a copy of this licence, visit <http://creativecommons.org/licenses/by/4.0/>.